TELESOUNDING,
A METHOD OF WIDE SWATHE DEPTH MEASUREMENT

by A.R. Stubbs, B.S. McCartney and Mrs. J.G. Legg
Institute of Oceanographic Sciences (*), Wormley, England

ABSTRACT

Telesounding is the name given to wide swathe measurement of sea-bed depths. The method described here is based on using a relatively simple side-scan sonar system having multiple beams. The principles of operation are discussed and the main sources of error shown to be sound refraction and transducer roll instability. Experimental versions have been built, tested and operated, examples of the records and analyses being presented. An immediate and permanent record is obtained which can be interpreted topographically by eye. Depths can be measured out to ranges between five and ten times the water depth, with errors generally less than 2 % of the water depth. Although coverage of the swathe with soundings is not uniform and the high data rate may present problems, the benefits include a twenty-fold saving of ship time. The method has applications in marine geology and, with development, for hydrographic surveys.

INTRODUCTION

Throughout maritime history the production of adequate charts showing the depth of the sea has been an important service for seafarers. Very early measurements may have been made by the use of a long pole in shallow water; later the lead and line became the universal tool. Many soundings on today's charts were obtained by lead and line. In shallow water, techniques were developed which enabled depth measurements to be made whilst the vessel was under way, but the ship's speed had to be low. Unfortunately when accurate measurements were required or where the water was over about 50 fathoms deep the vessel had to stop for each observation. *The lead and line is thus essentially a one dimensional instrument.*

The invention of the echo-sounder allowed the ship to take measurements while under way, with a consequent saving of survey ship time. Further, a permanent record is obtained so that the number of depth readings per line mile can be an order of magnitude more than for the lead and line method. Also, the pictorial cross-section of the sea bed provided by the record can itself be a useful guide to the geological nature of the sea bed. *The echo-sounder is essentially a two dimensional instrument.*

To contour a chart from sounding lines requires interpretative skill since there are usually gaps between the lines. The degree of uncertainty may be reduced for the cartographer by obtaining more closely spaced lines and by cross runs, but there is always a limit to the time and effort available and closely spaced lines call for a high degree of navigational precision.

Recently the advent of deeper draught vessels (CLOET, 1970; HAINES, 1970; RITCHIE, 1970b; van WEELDE, 1972) has imposed on hydrographers, both service and civil, a far greater workload. Previously it was only necessary, for example, to show that a channel was deep and to pinpoint the shallowest depths; now, depths are required over the whole width and length of the channel and the survey must be repeated more frequently to detect changes. The environmental penalties of stranded supertankers are obvious enough, so that the density of soundings must be adequate to ensure that obstructions are located. A great deal of money is spent upon dredging operations to keep shipping channels open and this work must be surveyed. Thus, the hydrographic effort required has increased due to the extension of :

(i)   areas to be surveyed;
(ii)   density of the soundings;
(iii) frequency of surveys;
(iv)   accuracy of soundings in deeper water.

An ideal situation would be to produce blanket depth coverage to port and starboard out to ranges exceeding the present line spacing, thereby increasing the data rate by an order of magnitude again and making more effective use of survey ship time. *The requirement is for a three dimensional instrument.*

Previous Work with Echo-sounders

The idea of a swathe of soundings has been put forward by a variety of authors (e.g. HAINES, 1970; RITCHIE, 1970a) and accompanied by a number of paper solutions (e.g. RITCHIE, 1970b; TUCKER, D.G., 1960). Practical work has been conducted in the main by extending existing techniques. The most obvious is the use of a number of echo-sounders whose transducers are arranged in a line athwartships. ENGELMANN (1967) and van WEELDE (1972) describe the use of paravanes to obtain lateral displacements of an extra two to four transducers. A higher density

over a narrower swathe has been obtained by FAHRENTHOLZ (1963) by the use of 25 transducers on outriggers on each side of the ship.

Another approach is to use a transducer arrangement which provides a number of beams directed at different angles from the vertical. This was first put forward by TUCKER D.G. (1960) and demonstrated by HOWSON and DUNN (1961). Lateral ranges to both sides of the ship and to distances rather less than the water depth could be obtained; one of the difficulties of this otherwise simple system was identifiying the beams; by making the beam sensitivities unequal TUCKER M.J. (1961) showed that beam identification could be simplified. Within-pulse, electronic, sector-scan sonars in the elevation scan mode avoid the beam identification problem, but are much more complicated systems and the cathode ray tube output presentation is less convenient than paper echo-sounder records (HOWSON and DUNN, 1961; MITSON and COOK, 1970). Sector-scan sonars are unrivalled for the obstacle and wreck location aspect of hydrographic work especially in the forward search mode (VOGLIS and COOK, 1966).

HICKLEY (1966) and GLENN (1970) describe other multibeam systems, which, though complex, are operational on U.S. ships; in these, the beam-forming networks generate separate outputs which are then connected to an equal number of signal processors which each gate, recognise and time the sea-bed echoes; beams within the sector ± 45° from the vertical are available. A similar or slightly larger sector is covered by a rather different system developed by Marconi-Elliott (CROWTHER, 1973); wide-band, wide-beam sound is transmitted and the sea bed echoes are received on two parallel, line hydrophone arrays spaced horizontally; their outputs are cross-correlated by a special purpose digital processor, which effectively generates beams at different angles and then gates and times the sea bed returns for each beam.

All the above multibeam systems are workable in the deep ocean, where typical sectors of ± 45° give a very useful ± 2.5 mile swathe about the track. In fact there is a very good reason in deep water why wider sectors become impractical; this is due to the inevitable refraction of sound by the non-uniform vertical sound speed profile.

When wide-swathe sounding on the continental shelf is considered, especially the estuarine and inshore areas, sectors of ± 45° give completely inadequate swathe widths of only tens of metres, whereas ranges out to about ten times the depth are required. The latter coverage is the same as that provided by side-scan sonar and it is natural to look to that method for alternatives. Indeed, the side-lobes in the vertical plane of such sonars have at times been used to calculate the depths of features to one side of the track, and have frequently been used to provide a qualitative picture of the topography (BELDERSON et al., 1972). Another effect which has occasionally been observed during calm weather on side-scan sonographs is the modulation of the pictures in alternate light and dark bands, orientated substantially parallel to the track. These bands are parallel to one another when received from a flat sea floor, but, when topographic features are present, deviate in sympathy with their rise and fall. Investigations (HAINES, 1963) indicated that an interference effect was taking place as a result of the reflection of sound from the sea surface.

This became known as the Lloyd-Mirror effect due to its similarity to the optical phenomenon. CHESTERMAN *et al.* (1967), and HEATON and HASLETT (1971) have shown how depth profiles may be extracted from Lloyd Mirror fringes on sonographs and indicate some of their limitations. GREISCHAR and CLAY (1972) extended the method and produced a contour chart, taking account of ray path distortion due to non-isothermal water.

The main disadvantage of the natural Lloyd Mirror effect, for any practical survey system, is that it does not occur often because the sea surface is too rough and the reflected sound is incoherent. One possible solution is to provide a plane acoustic reflector over the transducer to produce the Lloyd Mirror effect independently of sea state and, therefore, of season and location. Calculations by the present authors showed that with minor limitations this was feasible. Further, a roll stabilised, ship-mounted, side-can transducer already existed on R.R.S. *Discovery* which could be used as a convenient test platform. The project was put in hand and given the name " Telesounder ", implying depth measurement at a distance from the ship. An alternative solution investigated by the authors is to remove the plane reflector and use another line transducer located in the position of the ' image ' transducer. This arrangement may now be considered to be a two-element array with the well known multiple-beam diffraction or interferometer pattern. In this form the telesounder is very similar to the interferometer of HOWSON and DUNN (1961), but turned to work sideways instead of downwards. Any of the other systems mentioned above, which operate over $\pm 45°$, may in principle be tilted to cover $0°$ to $90°$ on one side, and sector-scan records of sea bed profiles have been obtained in this way.

Our reason for working on the telesounder as reported in this paper is our belief in the simplicity of this multiple beam, side-scan sonar method and its economy of transducers. Further the advantages of this system are that all the beams are recorded permanently on the same paper chart, are separable by virtue of the geometry, present an immediately recognisable picture of relief and may be converted to contour plots in a relatively straightforward way.

PRINCIPLES OF OPERATION

Production of Lloyd Mirror Fringes

The principle is illustrated in fig. 1 where the pressure release reflector, length L, is used. The point F on the sea floor receives sound from two directions, the first, direct from the transducer, along TF and the second along TMF after reflection. The reflected path may be replaced by T'MF, since TM = T'M, where T' is an image transducer. At M the soundwaves experience a $180°$ phase change so that when the path length difference at F equals an odd number of half wavelengths re-inforcement

of the sound takes place, and conversely, cancellation occurs for path differences equal to even half wavelengths. Thus as the pulses of sound travel out over the sea floor insonification takes place in bands. These bands give rise to echoes and from F one pair will be returned to the transducer along the routes FT and FMT and, since these have an odd half wavelength difference, the echoes will re-inforce on the transducer. The pressure amplitude of the phase coherent sound is thus double that received by normal echo-ranging. The loci of points having constant path length differences giving cancellation or re-inforcement are a series of hyperbolae with the transducers T and T' as their foci. Negligible error is introduced in practice by taking the asymptotes of the hyperbolae as loci; this is equivalent to a ' far-field ' approximation, for which FT and FT' are parallel rays. The condition for the point F to be in an enhanced beam is

$$\left(n - \frac{1}{2} \right) \lambda = d \sin \theta_n = d \, Z_n / R_n$$

where n is an integer assigned to that beam, λ is the wavelength of sound at the operating frequency and the other parameters are defined in fig. 1.
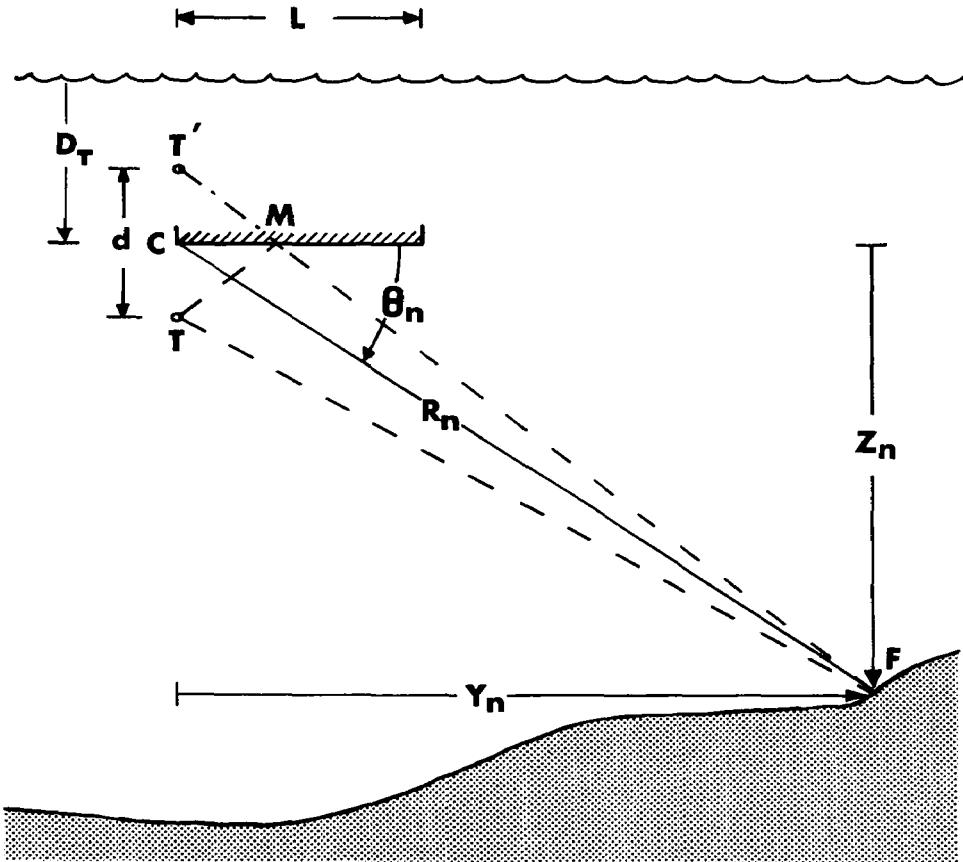
FIG. 1. — The Lloyd Mirror principle applied to a reflector and transducer, or to two transducers.

Let N be the number of beams in a quadrant and $\theta_N = 90°$ so that

$$\left(N - \frac{1}{2}\right) = d/\lambda \tag{1}$$

N is a constant for any transducer but need not be an integer, since d need not be an odd number of half wavelengths. Then we can write

$$\sin \theta_n = \left(n - \frac{1}{2}\right) / \left(N - \frac{1}{2}\right) \tag{2}$$

$$\cos \theta_n = \left\{ 1 - \left(n - \frac{1}{2}\right)^2 / \left(N - \frac{1}{2}\right)^2 \right\}^{\frac{1}{2}} \tag{3}$$

$$Z_n = R_n \left(n - \frac{1}{2}\right) / \left(N - \frac{1}{2}\right) \tag{4}$$

$$Y_n = R_n \left\{ 1 - \left(n - \frac{1}{2}\right)^2 / \left(N - \frac{1}{2}\right)^2 \right\}^{\frac{1}{2}} \tag{5}$$

The reflector length, L, is finite and so the lowest angle beam that is formed, numbered m, is given approximately by

$$\left(m - \frac{1}{2}\right) L \simeq d \left(N - \frac{1}{2}\right) / 2 = d^2 / 2\,\lambda \tag{6}$$

This limitation does not occur when a reflector is not used and a real transducer placed at T'. With this arrangement the transducer outputs may be subtracted (antiphase) or added (inphase); in the antiphase case the formulae (1)-(5) apply again; in the inphase case, which also applies for a reflector that is acoustically ' hard ', the terms $(n - 1/2)$, $(N - 1/2)$, $(m - 1/2)$ in all the formulae are replaced by n, N and m respectively.

Directivity Functions

Whatever system is used to obtain the interference effect it may be converted to a two transducer acoustic equivalent. The far field amplitude response as a function of angle is given by the directivity of one transducer multiplied by a function derived from the spacing between the two transducers — see, for example, ALBERS (1965).

For antiphase systems

$$A_a = \frac{\sin T}{T} \cdot \frac{\sin 2S}{2 \cos S} \tag{7}$$

and for inphase systems

$$A_p = \frac{\sin T}{T} \cdot \frac{\sin 2S}{2 \sin S} \tag{7a}$$

where

$$T = \frac{\pi a \sin \theta}{\lambda} \quad , \quad S = \frac{\pi d \sin \theta}{\lambda}$$

and a is the transducer width.

Fig. 2 is a computer plot derived from equation (7) for the two transducer array shown in fig. 4. The envelope containing the beam maxima is produced by the first term, the transducer directivity, and the
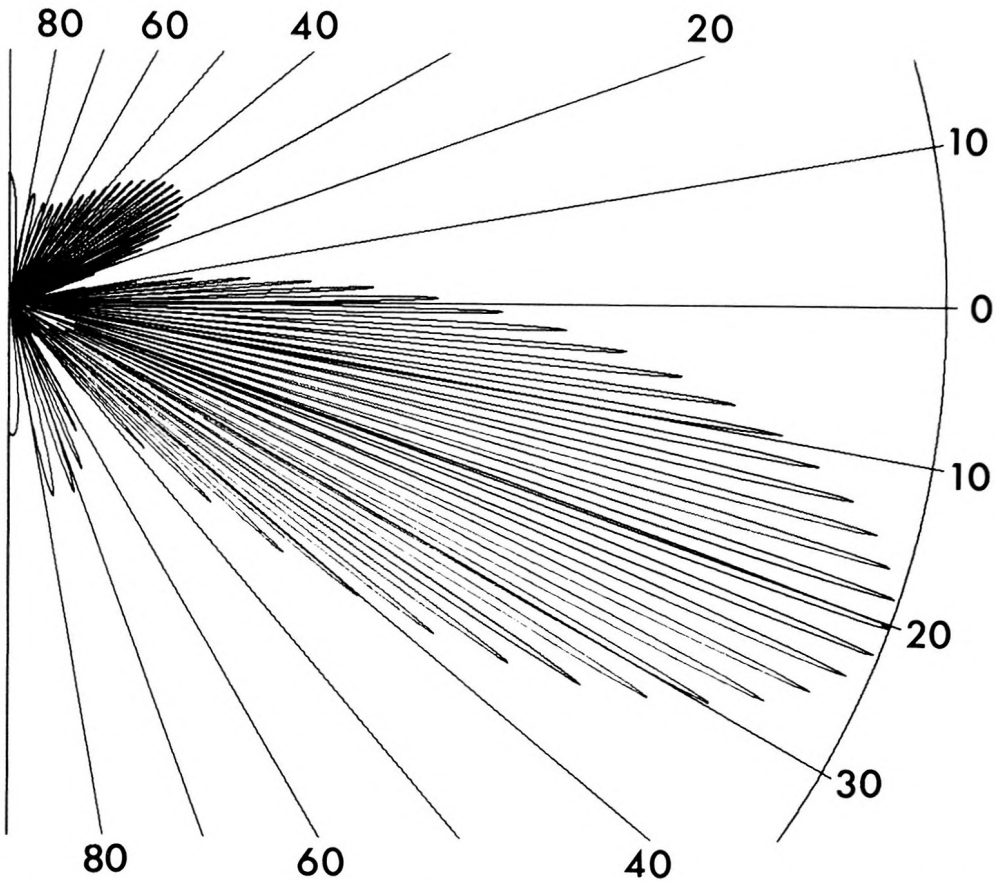
FIG. 2. — Directivity pattern of the two transducer array drawn on a linear amplitude scale.
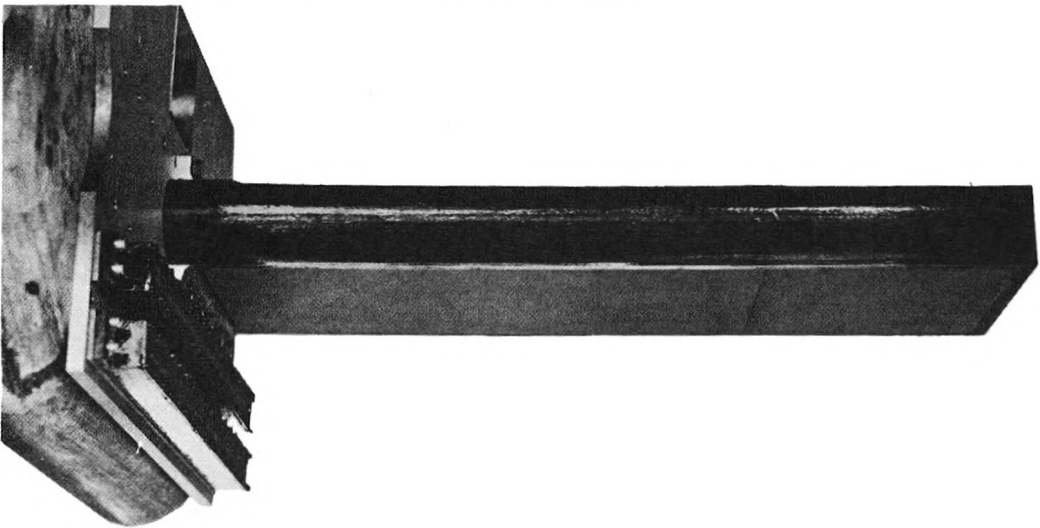
FIG. 3. — The reflector system with two transducers. The lower transducer is T_1. Reflector length 1 m, transducer lengths 65 cm.
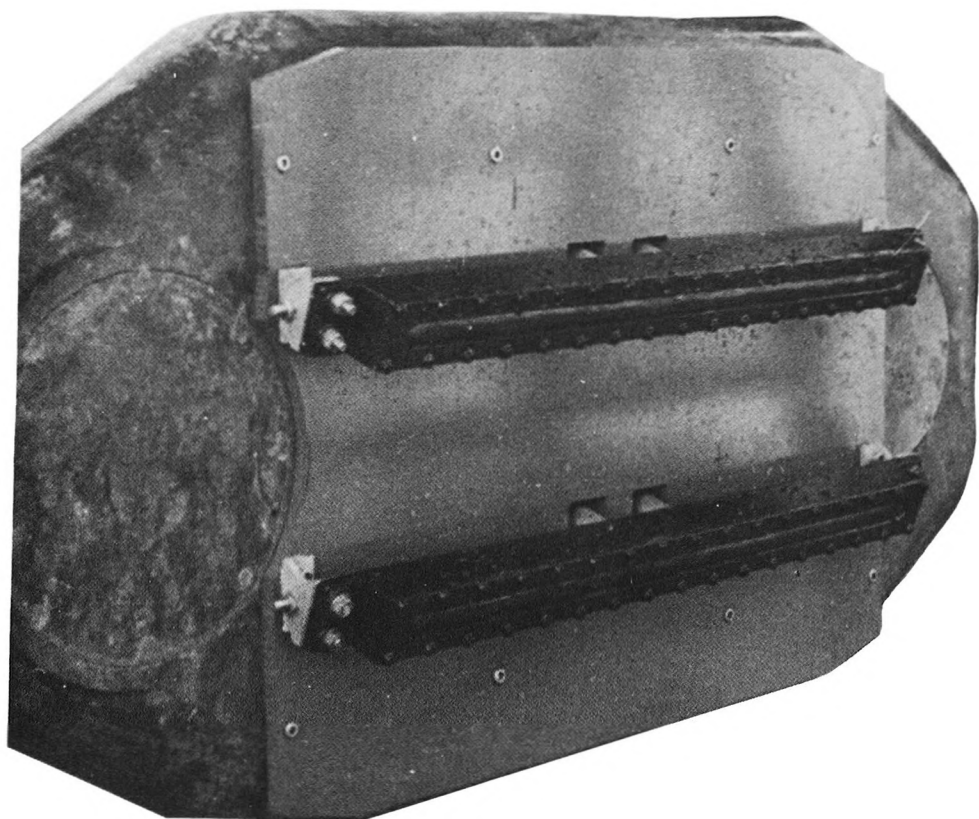
FIG. 4. — The two transducer array mounted on the back of the side-scan assembly.
Transducer separation 20 cm.

number and spacing of the beams is determined by the second term,
the spacing function. It will be noticed that in addition to the minima
between the beams there is a wide minimum on each side of the main
envelope. These are present because the width of each transducer is
greater than a wavelength; this is not a desirable characteristic, but was
tolerated in the absence of more suitable transducers.

Rotation of the transducers.

The main set of beams in fig. 2 has its envelope maximum angled
down; this is produced by rotating the individual transducers relative
to the line TT' by an angle γ, in this case equal to 20°. In equations (7)
and (7a), T becomes :

$$T = \frac{\pi a \sin (\theta - \gamma)}{\lambda}$$

Rotation enables maximum sensitivity to be employed at maximum range
and γ must be a compromise depending on the range of depths to be
surveyed. If the individual transducers have almost omnidirectional
patterns the narrow beams will have nearly equal amplitudes and rotation
will have almost no effect. In this case a will have to be 0.25λ or less,
which at high frequencies is mechanically difficult to achieve.

It should be noted that rotation cannot be used with reflectors. Here the directivity pattern must be symmetrical about an axis parallel to the reflector face because the sensitivity of the transducers in the directions of TF and TM must be equal or nearly equal.

Tilting of the array.

This is an operation whereby the transducer array is revolved about an axis at C so that the reflector or array normal is at an angle α to the horizontal.

It would appear at first sight that tilting is the same as rotation. However rotation changes the amplitude of a given beam without changing the position while tilting has the opposite effect. Tilting is used to vary the spacing over a given portion of sea floor, since the angular spacing of the beams increases with the beam number. In equations (2) and (3) above, θ_n becomes $(\theta_n + \alpha)$ with tilting and equations (4) and (5) become :

$$Z_n = R_n \left[\left(\frac{n - \frac{1}{2}}{N - \frac{1}{2}} \right) \cos \alpha + \left\{ 1 - \left(\frac{n - \frac{1}{2}}{N - \frac{1}{2}} \right)^2 \right\}^{\frac{1}{2}} \sin \alpha \right] \qquad (8)$$

$$Y_n = R_n \left[- \left(\frac{n - \frac{1}{2}}{N - \frac{1}{2}} \right) \sin \alpha + \left\{ 1 - \left(\frac{n - \frac{1}{2}}{N - \frac{1}{2}} \right)^2 \right\}^{\frac{1}{2}} \cos \alpha \right] \qquad (9)$$

The expressions in square brackets are calibration factors for each beam which only need to be re-calculated if α is changed.

Beam Identification

The expressions for calculating Z_n and Y_n involve the range R_n of the particular point on the sea floor and n the number of the beam producing the fringe. Now n is an integer and an error in this parameter will give a gross error in depth, so correct identification is essential. There are various methods for achieving this depending on the array employed. Having determined the value of n for one beam the values for the others follow sequentially.

Known depth.

This is a fairly obvious method, the value of the depth at the known feature being entered into equation (4) together with the corresponding range and the number of the beam producing the echo is obtained. This

method is most sensitive for small values of n and an echo-sounder run at right angles to a telesounder run is a convenient tactic.

Flat sea floor.

CHESTERMAN *et al.* (1967) have demonstrated that when the sea floor is substantially flat, by plotting $1/R_n$ versus an arbitrary fringe number sequence, a straight line is obtained, from which the complete calibration factor can be determined, even in the case of a towed transducer at an unknown depth from the reflecting surface.

Minimum number beam of reflector array.

The record beyond the mth fringe with a reflector array reverts to a normal side-scan picture. Thus if this region can be displayed and recognised, as in shallow water, or by tilting, beam numbering follows.

Alternative frequencies or spacings.

The total number of beams, N, is dictated by the spacing, d, and by λ, the wavelength. Thus an array can be made to have more than one set of beams by changing the frequency of transmission or by having alternative spacings. In the former case from equations (1) and (4) :

$$\frac{Z_n}{R_n} \cdot d = n_1 \lambda_1 = n_2 \lambda_2 \quad \text{for the inphase condition}$$

For example if 10 fringes of frequency f_1 occupy the same space as 9 fringes of frequency f_2 then $\lambda_1 = 0.9\, \lambda_2$ and $f_2 = 0.9\, f_1$; so for $f_1 = 250\,\text{kHz}$, f_2 would be $225\,\text{kHz}$. This frequency difference is feasible within normal transducer bandwidths.

On the other hand if λ is fixed and two pairs of spacings d_1 and d_2 are available,

$$Z_n / \lambda R_n = n_1 / d_1 = n_2 / d_2$$

The spacings are only limited by the space available, and a wider variation than for frequency is practical. By switching from one pattern to the other an inspection of the record will indicate the required co-incidence, as demonstrated later for fig. 6.

An alternative method is to use both transducers together, thereby generating a completely different but characteristic directional pattern. This is demonstrated also in fig. 6 for a short strip in the centre. At a range of 150 m a beam strikes the sea floor for all three transducer arrangements, allowing an unambiguous determination of fringe numbers.

Beam pattern irregularities.

For a perfectly designed array the amplitude of the individual beams will vary smoothly according to the function sin T/T. However, it will

be seen in fig. 12, for example, that this is not quite so in practice, certain fringes being more dominant. The darkest fringe at the shorter range was established to be No. 22 by the flat sea floor technique, and from then on it was only necessary to pick out this darker fringe to establish the complete pattern. (This was confirmed later by obtaining a measured directivity pattern.) This variation of intensity from beam to beam is due to additional reflections onto the transducer from the base plate. These will vary with angle of incidence both to the plate and also to the back of the transducer. The effect is small because the backward directivity of the transducer is low.

Pulse Length

The minimum pulse length must be long enough to produce at least 1 cycle overlap on the last beam when $n = N$.

The minimum pulse duration $\tau_m \geqslant N\lambda/c$.

Now $N = d/\lambda$ or $N = d/\lambda + 1/2$ and $N \gg 1/2$.

Therefore $$\tau_m \geqslant d/c \qquad (10)$$

where c is the velocity of sound.

Thus the pulse length in water must exceed the transducer spacing. Usually, to obtain a good coherent output, at least 10 cycles overlap is required.

The maximum pulse length condition also occurs at $n = N$ and is a function of water depth. The pulse should ideally be short enough to separate the echo returns from the Nth and the $(N-1)$th beams. Let τ_M be the maximum pulse length, then

$$c\,\tau_M \leqslant R_{N-1} - R_N$$

$$\leqslant Z_{N-1} \cdot \frac{N}{(N-1)} - Z_N \quad, \text{ for the inphase condition}$$

Normally : $\qquad Z_N \doteqdot Z_{N-1}$

Therefore : $\qquad c\,\tau_M \leqslant Z_N \left(\frac{N}{N-1} - 1 \right) = Z_N/(N-1) \doteqdot \frac{Z_N}{N}$

But : $$N = d/\lambda$$

Therefore : $$\tau_M \leqslant \frac{Z_N}{c} \cdot \frac{\lambda}{d} \qquad (11)$$

It is apparent that at shallow depths there is a conflict between these two limits and an empirical compromise must be adopted. In any event it is the angular region near the vertical which is affected one way or the other, whilst it may be noted that the major proportion of the swathe width is provided by angles $\theta_n < 45°$.

EXPERIMENTAL EQUIPMENT

The side-scan transducer used on R.R.S. *Discovery* is built into a casting held on trunions between two fore and aft legs attached to the underside of a horizontal plate which becomes part of the ship's hull when installed. The transducer is then 1 m below the ship and about 6 m below the sea surface. The array may be tilted in the roll direction by means of a motor inside the ship via a shaft inside the after leg; roll servo-stabilization is also achieved with the same motor drive. The transducer is single sided and so the back of the casting is an ideal platform upon which to mount experimental telesounder assemblies.

Transducer/Reflector Assembly

The reflector assembly is shown in fig. 3. A thick metal plate is bolted to the back of the casting and on this is mounted the reflector and two transducers. Two transducers are used to obtain two sets of beams to aid beam identification. The reflector is a hollow bronze casting with fairings on the leading and trailing edges, and unicellular rubber is glued to the underside to provide the pressure release surface. Only one half the length of each transducer is covered by the reflector because there are two separate sets of transducer elements in each housing which allows the other halves to be used for ordinary side-scan work.

Two-Transducer Assembly

For the two transducer system the metal plate of fig. 3 has been replaced by a tufnol plate in fig. 4 and the lower transducer of fig. 3 has been moved up to occupy the position of the virtual transducer. Also, both transducers have been rotated downward about their axes, as discussed above.

Operating Parameters

Frequency of transmission	250 kHz
Wavelength λ	0.6 cm
Horizontal beam width	1°
Vertical beam width	35°
Total output power	70 Watts
Pulse length τ	0.4 ms

Reflector assembly :

Reflector length L	92 cm
Reflector width	30 cm
Upper transducer — reflector distance $d/2$	10 cm
Maximum number of beams N	33.8
Minimum beam number m	5
Lower transducer — reflector distance $d/2$	18 cm
Maximum number of beams N	60.5
Minimum beam number m	13

Two transducer assembly :

Transducer separation d	20 cm
Maximum number of beams N	33.8
Rotation angle γ	20°

Electronics and Display

The signal circuits are entirely conventional side-scan circuits including the provision of time varied gain on reception. The output is displayed on an 11″ Mufax wet paper recorder having a sweep rate of 3 per second giving a recorder range of 250 m.

SONOGRAPH INTERPRETATION

The telesounder system is an extension of side-scan sonar and so it is not surprising to find the two displays have similar formats. For example in fig. 5 the ship's track is from left to right along the top of the record and the undulating dark line immediately below is the sea bed profile directly under the ship. Further, echoes from features out to the side of the ship's track are displayed at the appropriate ranges as for conventional side-scan sonographs. The difference between the two being that whereas for ordinary side-scan systems the main beam provides a continuous picture over the major portion of the record, the telesounder display is broken up into a series of bands or fringes which increase in width and spacing as the range increases. These fringes change range in sympathy with the topography, an increase in range signifying an increase in depth and *vice versa*. The general appearance of such sonographs is to give a three dimensional impression of the topography even before any quantitative analysis is undertaken. The pictorial effect may be enhanced by tilting the top edge away and viewing the sonograph obliquely at a shallow angle.

Fig. 5 was obtained by using the reflector and upper transducer of fig. 3. Features longer than the fringe spacing can be followed across the record, for example the white shadows on the right hand side, due to steps in the sea floor; also features smaller than a fringe width, usually textural changes, are easily observed, for example within the wide fringe toward maximum range. The overall change of slope along the record is easily detected but it should be noted that this is not so for slope across the record. The saw tooth type perturbations of the fringes which are coherent across the record for all beams are caused by the unstabilised state of the array while this record was being recorded. The regular series of dashes on the lower part of the record is interference from an echo-sounder.

Fig. 6 was also obtained using the unstabilised reflector array over a fairly flat sea floor and shows the effect produced by switching trans-ducers. On the left, transducer T_1 is used alone, and likewise transducer T_2 on the right. The band in the middle is the result of using the two transducers together to produce a secondary interference pattern. By noting coincident beams, and with the knowledge of the array parameters, the beam number may be allocated with certainty. For this array the possible coincident pairs of beams occur as follows :

n_1	5	14	23	32	41	50	59
n_2	3	8	13	18	23	28	33

The first pair do not exist due to the finite length of the reflector so the first useable pair are numbers 8 and 14 and these occur coincident with the first dominant fringe of $(T_1 + T_2)$ working in from extreme range. Reducing the range further for $(T_1 + T_2)$ a pair of equally dominant fringes can be seen. However these do not coincide exactly with a fringe of T_1 or T_2, but the next dominant fringe of $(T_1 + T_2)$ may be used to check that $n_1 = 23$ when $n_2 = 13$.

The remaining sonographs in this section, figs. 7-11, were obtained using the two transducer array, fig. 4.

Fig. 7 demonstrates very clearly the pictorial effect mentioned above as the beams move over the undulations of two large sand waves. Beam number allocation is carried out by noting the dominant fringe, produced by beam 22, and counting each way. The rough sea experienced at the time is evidenced in three ways. Firstly, by the numerous sea wave echoes at short range (the absence of a reflector will allow a greater number of these echoes to be received); secondly, the short period per-turbations of the fringes caused by incomplete stabilisation and heave effects and finally, by the continuous trace on the lower part of the record. This thin sinuous line is a measure of the heave of the trans-ducer for this record, and the maximum vertical displacement is 1.2 metres.

Fig. 8 shows a series of asymmetric sand waves recorded in fairly calm weather as suggested by the heave meter record. Fringe 22 is not so dominant but is still apparent. The minute perturbations of the fringes could be assumed to be due to ship motion; however, it will be noted there are increases of amplitude occurring on the upper regions of the large

sand waves. It is concluded that these are due to small sand waves about 1.4 metres high whose crests are substantially parallel to the main crests. It will be noted also that there is evidence of very small sand waves in the trough on the extreme left. From this record it is not possible to obtain the heights of these very small sand waves except to say they must be less than 30 cm high.

Fig. 9 is a sonograph of almost symmetrical sand waves with sharp crests and an area of variable grain size as indicated by the patchy varia‑ tion of texture. Fringe 22 is weak in places, but can be checked by following along from adjacent areas. The other interesting features on this sonograph are the dark bands displayed across the record and asso‑ ciated with the crests of the sand waves. These are the result of noise produced on the sea floor by the movement of particles on the peaks of the sand waves (VOGLIS and COOK, 1970). In the middle of the record the telesounder transmissions were switched off but the transducers were still in use as receivers; the two noise bands that appeared occurred simul‑ taneously with two peaks on the ship's echo-sounder. Note also that the bifurcated sand wave on the right has two noise bands emanating from points which are not under the ship but at least 100 m away. The noise, being continuous, does not produce fringe patterns on the record.

Fig. 10 might at first sight appear to be a conventional side-scan sonograph of a complex sand wave region in shallow water. Closer inspection, however, reveals that fringes are present and that the heave of the ship, of up to $1\frac{1}{2}$ m, adds to their displacement. The picture is made more complex by the variety of sand wave sizes present and by their variable trends. At short ranges the spacing of the beams on the ground is smaller than the sand wave spacing, at longer ranges the reverse is true and at some intermediate range the two are of equal size and it is impossible to resolve them. Beam identification and numbering are not easy to carry out but it is estimated, nevertheless, that about 40 % of the record could be analysed with care and patience. Some noise bands are present on the right side of the sonograph, while the series of dashes along the middle of the record is due to interference from an echo-sounder.

Fig. 11 was obtained during bad weather over a flat sea floor in deeper water. Fringe 22 is easily picked out right along the record and detection of other fringes only presents difficulty in some of the lighter toned areas. These light toned areas are probably sand, the adjacent very dark patches are possibly gravel and the striated regions between are areas of small sand waves. The boundaries between the areas were examined carefully in an attempt to detect steps. However none were found indicating that any height differences are less than 30 cm. A fish shoal on the right of the sonograph casts a long shadow on to the sea floor. Calculations indicate the shoal is about 20 m across, lying 60 m deep and 60 m away from the ship. The fish shoal does not exhibit a fringe pattern because its front face is too steep.

THE PRODUCTION OF DEPTH CONTOURS

To produce contoured plots from a sonograph the following stages of analysis were performed, a portion of fig. 12 being used as an example and fig. 13 the final product.

First, a traced overlay of the record was produced in which the transmission zero, and the best estimate of the centre of each recognisable fringe was traced between two times, in this case from $2037\frac{1}{2}$ to 2039. From the navigational data the distance travelled in this $1\frac{1}{2}$ minute period was found and then the distance along the record equivalent to 10 metres of track calculated. The tracings of the fringes were labelled with the appropriate beam number.

Second, the traced overlay was placed upon a trace reader, in this case a DMac System II; the transmission mark was lined up along one co-ordinate, X, of the trace reader and the other co-ordinate, Y, proportional to R_n, set to zero. The trace reader was set to sample the Y value for each increment in X, equivalent to the 10 metre spacings as calculated above. Each fringe was carefully followed whilst the punched paper tape output logged the regular series of R_n values. This was repeated for every fringe, each tape sequence being preceded by its defining value, n. The paper tape was edited to include the fixed parameters α, d, λ, sampling interval and the start and finish times.

Third, the edited paper tape was fed into a computer, which initially calculated the calibration factors for the first beam, as given by the square brackets in equations (8) and (9); the depth Z_n and horizontal position Y_n were then computed; finally a three digit figure of the depth in decimetres was written centrally at the position (X, Y_n), for each increment in X, on a drum plotter to a true X, Y scale of 1 cm to 10 metres (i.e. 1/1000 scale). The other fringes in turn were treated similarly.

The final operation of contouring the depths at one metre intervals was done manually, to produce fig. 13, representing an area 550 m by 200 m.

Obviously this whole analysis procedure took considerably longer than the $1\frac{1}{2}$ minutes required to obtain the record at sea, though perhaps no longer than the analysis of a conventional echo-sounder survey providing the same number of depth samples, but using perhaps twenty times as much ship time. The analysis could be speeded up considerably, for example by using a small dedicated computer whose input is linked directly to the trace reader and whose output is coupled directly to a fast visual display device. The digitizing might possibly be taken directly from the record in many cases, eliminating the tracing sheet. However, it is believed that this stage can be useful as it separates the detection and measurement. Also it might be possible to produce the tracing so that subsequent optical or magnetic digitising could be automatic.

Simple Method for Limited Analysis

For some applications the full analysis procedure may not be required, it being sufficient to use only a proportion of the total number of beams, or else only the depths of the peaks need be determined. Simple scales were produced and overlayed on the record for each point in turn and the values of Z_n and Y_n read off directly. This system was slightly tedious, but plastic scales in a purpose built frame can provide a practical method of manual analysis.

ERRORS

The use of telesounder is based on calculations which give the total water depth in the form

$$D = D_T \pm h + \frac{ct_n}{2} \sin \theta_n$$

where D is the total water depth, h is the instantaneous value of the ship's heave and t_n is the travel time along the nth beam. The sources of error in the system may thus conveniently be placed into three independent groups, namely ship motions largely affecting θ_n and h, the recording and analysis system affecting t_n, and environmental data, affecting knowledge of c and θ.

Errors due to Ship Motions

Any uncompensated roll can introduce errors because the reference for θ_n is no longer the true horizontal. All the beams are rotated similarly, but depth errors will be more serious at low values of θ_n, that is at long range, whilst errors in horizontal position will be most serious when $\theta_n = 90°$, at close range. If for the moment we assume that the maximum range Y is about ten times the water depth we require a minimum $\theta_n = 5.7°$, so this angle and 90° are used as limiting values in the tables below. The first table shows the errors δZ_θ and δY_θ in depth and lateral range respectively, due to using the nominal beam angle θ_n instead of $(\theta_n + \delta\theta)$.

$\delta\theta$	$\pm 2°$	$\pm 1°$	$\pm 30'$	$\pm 15'$	$\pm 7.5'$
$\delta Z_\theta / Z_n$ (at $\theta_n = 5.7°$)	+ 0.26 − 0.54	+ 0.15 − 0.21	+ 0.080 − 0.096	+ 0.042 − 0.046	+ 0.022 − 0.022
$\delta Y_\theta / Z_n$ (at $\theta_n = 90°$)	± 0.035	± 0.017	± 0.0087	± 0.0044	± 0.0022

Roll, therefore, has a far more serious effect on the accuracy of depth
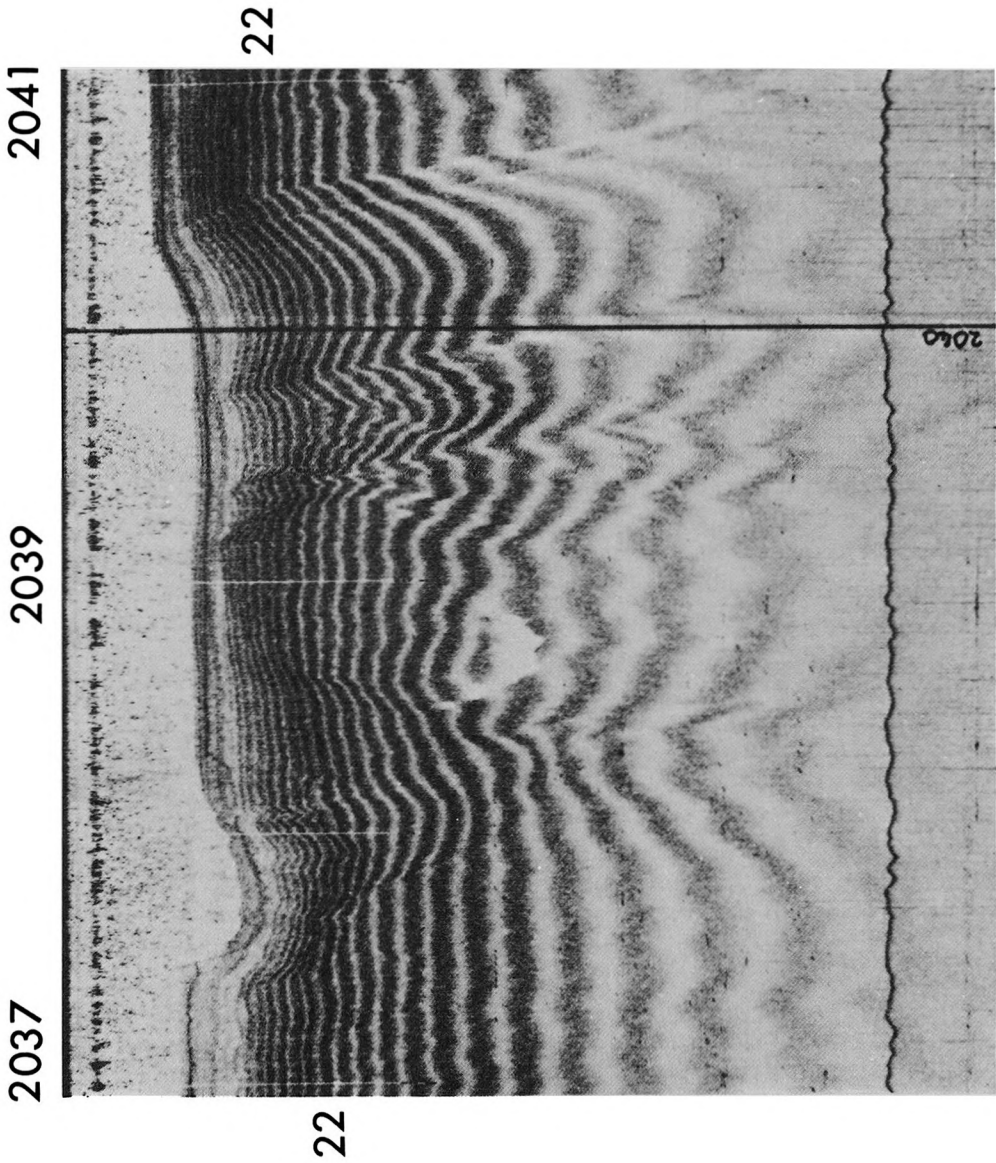
FIG. 12. — An undulating sea floor in the Straits of Dover.
The contoured analysis of the region between 2037½ and 2039 is shown in Fig. 13.
Length 1100 m, width 250 m, water depth 24-49 m.

than of position. With a towed body roll stabilities within $\pm 1°$ may be possible, but anything better would probably be quite difficult. For a ship-mounted system, stabilisation to within $\pm 1°$ is not too difficult to obtain, to achieve $\pm 15'$ would need considerable care whilst to achieve $\pm 7.5'$, though feasible, would require a very expensive gyro system. To ensure exact and continuous recognition of the beams *some degree of roll stabilisation is essential for all quantitative work.*

Uncompensated deviations in pitch angle, $\delta\Phi$, cause errors in all three co-ordinates δZ_p, δY_p and δX_p, where X is the co-ordinate along the track of the ship, as shown in the next table.

$\delta\theta$	$\pm 10°$	$\pm 5°$	$\pm 2°$	$\pm 1°$
$\delta Z_p/Z_n$	0.015	0.0038	0.00061	0.00015
$\delta Y_p/Z_n$ (at $\theta_n = 57°$)	0.15	0.038	0.0061	0.0015
$\delta X_p/Z_n$	± 0.17	± 0.087	± 0.035	± 0.017

Errors in lateral position are worse at long range and, as the table indicates, positional errors are greater than depth errors.

Vertical displacement of the transducer due to ship heave and pitch shifts the reference depth D_r. This is probably difficult to compensate mechanically, and unlike an echosounder cannot be compensated by delaying the pulse transmission relative to the recorder sweep, because the change in travel time is different for each beam. By integrating twice the output of a vertical accelerometer, the vertical displacement may be logged or, as in our experiments, displayed on the records. The resultant displacement trace, which can be seen on figs. 7, 8, 9, 10 and 12, may be digitised and stored at the same time as the beam traces.

Deviations in the heading of the ship from the course made good, due to set and yaw, do not introduce depth errors but do cause positional errors. This has been considered and corrected by HOPKINS (1970) for the purposes of producing a mosaic of side-scan sonographs. Corrections for set, yaw and sway are dependent upon having good navigational data, but can be straightforward to apply at the plotting stage. The achievement of accurate navigation, though vital to surveys using telesounder type equipment, is considered to be beyond the scope of this paper.

The ship motions and resultant errors have been simplified by separation above so that a feel may be obtained for the magnitudes of the errors. In practice all motions will be present simultaneously and, depending upon the particular ship and the sea, there may be coherence between these motions.

It is evident from the records that in many cases the spatial scale of the sea bed features are larger than the perturbations due to ship motion; it is then tempting to smooth out the perturbations by eye when the operator digitises the traces. This may be permissible for small motions, but because the errors are non-linear and asymmetric can lead to biased readings.

Errors due to Recording and Analysis

The two-way travel time, t_n, of the nth beam is measured as a length from the record and any errors in it introduce proportionate errors in Z_n and Y_n. Because the width of each beam trace on the record is finite, there is a choice between taking the centre of the trace or the position of maximum intensity for t_n. The former may be preferred since the maximum is flat topped and with many recorders difficult to discern; however the edges of the beam trace are not sharp and the marks will be asymmetrical about. θ_n, due to the sin θ_n dependence of the directivity function argument. Taking, for algebraic convenience, an inphase, two-transducer system it can be shown that over a flat sea floor the half amplitude points of the nth beam strike the sea bed at times $t_n - t_n/(3n-1)$ and $t_n + t_n/(3n+1)$. Let Δt_n be the difference in travel times of the half amplitude points of the beam, and δt_n be the offset from t_n of the mid-point of the half amplitude points. Then

and
$$\Delta t_n/t_n = 6n/(9n^2 - 1)$$
$$\delta t_n/t_n = 1/(9n^2 - 1)$$

For the lower values of n, that is the longer ranges, one might reasonably expect to judge the centre of the beam to within about $\pm 0.1 \Delta t_n$, and from the table below it can be seen that this will generally exceed the offset or bias due to asymmetry.

n	1	2	5	10
$\delta t_n/t_n$	0.125	0.029	0.0045	0.0011
$0.1 \, \Delta t_n/t_n \; (= \delta Z_t/Z_n)$	0.075	0.034	0.013	0.0067

For higher n values, that is the close range beams, the resolution of the trace reading process, including any intermediate line tracing stage if used, becomes the limiting factor. A resolution of 1/500th full scale recorder width is feasible and generally the water depth will be about 1/10th of full scale so that in this region $\delta Z_t/Z_n$ should not exceed 0.02.

Other causes of asymmetry in the fringes on the record could be variations in spreading loss and backscattering across the beam. It is assumed that the difference in spreading loss across the beam due to range differences is counteracted by the time varied gain. The variation of backscattering with angle for many sea bed types is rather small especially in the range $\theta < 70°$ (McKINNEY C.M. and ANDERSON C.D., 1964), and so it too may be disregarded as a source of asymmetry.

These idealised error calculations assume that the sea bed reverberation levels exceed the noise level. Ideally too, they apply to each pulse transmission, though accuracy of measurement is improved if there is high coherence from pulse to pulse, that is if the spatial scale of sea bed

features are larger than the beam spacings and pulse interval distance
along the track. Records become difficult to read when spatial scales are
comparable with beam spacings as in fig. 10. However when the scale
is very much smaller than the spacings, the beams will be recognisable
again and it is apparent that the measurements will represent an average
over the area of a resolution cell, given approximately by :

$$\Delta R \cdot \varphi \cdot R_n \cdot \cos \theta_n,$$

where φ is the horizontal beamwidth in radians, and if τ is the pulse
length,

$$\Delta R = c\tau/2 \quad \text{at long ranges.}$$
$$\text{and} \quad \Delta R = c\Delta t_n/2 \text{ at short ranges.}$$

As range increases the density of soundings reduces, the sampling
area for each independent sounding increases and generally the errors
increase.

A major source of systematic error is uncertainty in the tilt angle α.
If this is unknown, but stable, it may be determined as part of the
calibration process as described later for the Dodman Point Survey. Other-
wise the calculations for uncompensated roll, $\delta\theta$, apply also to tilt devia-
tions, $\delta\alpha$.

Errors due to Refraction

Sound rays are refracted towards regions of lower sound speed, which
is mainly dependent upon temperature, salinity and depth. Though abso-
lute variations in sound speed are quite small, generally less than 2 %,
the small angles of refraction have proportionally a large effect because
of the small grazing angles in use with telesounders. Temporal and
spatial variations in the environmental parameters due to seasonal heating,
tidal flow and internal waves for example all affect sound propagation, but
may need different methods of handling due to the differences in scale.
Internal waves do on occasions cause severe refraction distorsion on side-
scan sonars, analogous to looking through a bottle glass window; tele-
sounding in these conditions is impossible. Seasonal changes in mean
sound speed may be handled simply by changing the recorder sweep speed
or calibration factor. In between these two extremes it is apparent that
continuous monitoring of the environmental parameters may be required.
Then, depending upon the magnitude of the variations, it may be necessary
to make corrections for refraction, or limit the swathe width, or ultimately
abandon the survey until conditions improve.

It is generally assumed that horizontal stratification applies when ray
paths are computed using sound speed profiles. If this assumption is not
valid in practice then correction for refraction would be impractical.
There are several ways of approximating the profiles including multi-layer
models with constant speeds or constant gradients. The method for
illustrating refraction here is based upon theory developed by DAINTITH
(1970); the sound speed $c(Z)$ is known and characterised by $\bar{c}$, its mean

value to depth Z_n, and by its standard deviation, σ_v, to the same depth. Then to second order in $(\sigma_c/\bar{c})^2$:

$$Z_n = \frac{t_n}{2} \, [\bar{c}] \, [\sin \bar{\theta}_n] \, [1 + (\sigma_c/\bar{c})^2 \cdot f(\bar{\theta}_n)]$$

where :
$$f(\bar{\theta}_n) = \left(1 - \frac{1}{2} \cot^2 \bar{\theta}_n + \frac{3}{2} \cot^4 \bar{\theta}_n\right)$$

and $\bar{\theta}_n$, the mean angle of the nth beam is related by Snell's law to the initial projection angle θ_n and the sound speed, c_T, at the transducer, by

$$\cos \bar{\theta}_n/\bar{c} = \cos \theta_n/c_T$$

Since $\bar{c}$ and σ_c are the mean and standard deviation to depth Z_n, which is the dependent variable, an iterative process may be required. The three factors for Z_n in square brackets indicate that the sound travels at a different mean speed, a different mean angle and over a longer curved path than the straight ray initially projected. With full knowledge of c_T, $\bar{c}$ and σ_c, the values of $\bar{\theta}_n$, $f(\bar{\theta}_n)$ and $\sin \bar{\theta}_n$ could be calculated for each of the θ_n values, thereby generating the calibration factor for each beam. However it is worth considering the errors introduced by further simplifications.

Firstly, neglecting the last term due to variance, the depth errors δZ_v for a range of $(\sigma_c/\bar{c})$ values are shown in the next table.

$(\sigma_c/\bar{c})$	5×10^{-4}	10^{-3}	2×10^{-3}	5×10^{-3}
$\dfrac{\delta Z_v}{Z_n}$ (at $\bar{\theta}_n = 5.7°$)	0.0038	0.015	0.060	0.38

These errors reduce very quickly as $\bar{\theta}_n$ increases, becoming one tenth of the above at $\bar{\theta}_n = 10°$ for example.

Secondly, the difference between $\bar{\theta}_n$ and θ_n when the latter is $5.7°$, and the effect of ignoring this difference on the depth error δZ_v, is shown in the next table, for a range of $(c_T/\bar{c})$.

$c_T/\bar{c}$	0.998	0.999	0.9995	1.0005	1.001	1.002	1.005
$\bar{\theta}_n$ (at $\theta_n = 5.7°$)	4.402°	5.093°	5.405°	5.980°	6.247°	6.749°	8.067°
$\dfrac{\delta Z_v}{Z_n}$ (at $\theta_n = 5.7°$)	−0.29	−0.12	−0.054	0.047	0.087	0.15	0.39

c_T must be within 0.29 m/s of $\bar{c}$ to prevent errors more than $0.2 \, Z_n$ at maximum range.

Finally, as with a normal echo sounder, errors in calibration speed introduce proportional errors in depth.

In order to obtain some idea of how frequently refraction would be a problem, 365 sound speed profiles from mainly inshore and estuarine stations around the east coast of Britain were examined and $\bar{c}$ and σ_c calculated. Values of $\bar{c}$ varied from below 1460 m/s to above 1490 m/s, about 45 % of the profiles had standard deviations less than 0.2 m/s, about 90 % less than 3 m/s and the maximum standard deviation was 10 m/s.

This data is not necessarily truly representative either geographically or seasonally, but does indicate that often the variance term may be ignored, the mean angle correction less frequently, and the mean speed never.

Refraction will also cause errors in lateral position, and like errors in roll angle these will be worse at short ranges.

Repeatability of Telesounder Experiments

In order to obtain an estimate of the actual errors in practical situations, surveys were planned which included covering the same area of ground with crossing tracks. For these experiments it was necessary to have good navigation and Hi-Fix was hired for this purpose, using existing chains. On the first occasion the weather conditions prevented the ship entering the chosen estuarine survey area for which tidal measurements were available. Instead, the experiment was performed in rather deeper water (58 m) at 50°14′ N, 4°45′ W near Dodman Point over a nearly flat sandy sea floor, but tidal differences had to be estimated from tables. By choosing a flat sea-bed the demands placed on the navigation are not quite so severe, and in deepish water the angular range is not so great. A second survey was made in much shallower water (20 m) at 51°48′ N, 1°36′ E, in the outer Thames estuary at Long Sand Head, in an area of sand waves about 6 m high from peak to trough and with a crest-to-crest wavelength around 100 metres. For this second survey tidal measurements were available and a sound speed profile was taken.

For both surveys the data was analysed as described above and true scale charts of depth readings in decimeters produced with a sampling interval along the track of 10 metres, and identifying the beams by the darker fringe, number 22. The charts were then overlapped according to the navigational data and plots made of the differences in soundings between runs at all positions co-incident within about ± 2 m.

Dodman Point Survey.

It was evident by looking at the differences on one plot between the echo-sounding lobe of one run and the soundings with range of the other that there were range dependent errors. These were believed to be due to errors in tilt angle, α, rather than range R_n. These errors are $\delta Z\alpha$, where :

$$\delta Z\alpha / Z_n = \delta\alpha \cdot \cot(\theta_n + \alpha)$$

so by taking the echo-sounder readings as Z_n and the nominal values of $(\theta_n + \alpha)$ for the beams on the crossing track, graphs of $\delta Z\alpha / Z_n$ versus cot $(\theta_n + \alpha)$ should be a straight line with gradient $\delta\alpha$. This gave $\delta\alpha = 18'$ in one case and $\delta\alpha = -33'$ in the other. Now these angular errors are too small to be due to incorrect choice of n, and this would not give a linear distribution anyway, nor would an error in N. However there are several ways in practice for an error to occur in α. For the gyro used errors within ± 15′ can occur in the reference, the roll angle

control may only be read to within about ± 15′, it is estimated that backlash can contribute up to ± 20′, and finally an error of — 11′ was subsequently measured between the gyro platform and the transducer platform when the ship was stationary. Between the two crossing runs 2 hrs 28 mins elapsed, adequate time for the value of α to change through the above range. No sound speed data were available for this survey, made after a period of storm, which may have helped to reduce near surface gradients. Errors due to refraction however would not tend to give linear plots, nor would the polarity of the error be likely to change so quickly, though it is possible that refraction contributes part of the mean error of — 15′.

In each case the values of $(\theta_n + \alpha)$ were corrected by $\delta\alpha$ and the telesoundings re-computed and cross compared as before. There was now no systematic pattern in the difference apart from the mean difference of 1.85 metres, compared with an estimated tidal difference of 2.2 metres. The distribution of the 211 differences from an area covering 130 metres by 170 metres is shown in fig. 14 and the standard deviation is 0.4 metre. Since the mean depth was 52 metres below the transducer the telesounder appeared to be repeatable on this occasion within the range $\delta Z/Z = \pm .023$ (± three standard deviations).

Long Sand Head Survey.

The sound speed profile gave $(\bar{c} - c_T)$ less than 0.2 m/s and $\sigma_c = 0.07$ m/s so that errors due to refraction were small. Determination of $\delta\alpha$ for the two crossing profiles gave + 6′ and + 42′, but with much poorer correlation than for the Dodman Point survey. The reason for this is probably that navigational errors, and the subsequent misalignment of the plots, introduced apparent depth differences over this uneven sea bed. Lining the plots up by the trend of a sand wave peak suggested errors in position of the order of ± 5 m, which in the steepest region could give a 0.5 m depth difference. The distribution of 121 differences from positions spread over an area of 70 m by 90 m is shown in fig. 15. The standard deviation in this case is 0.13 m and the mean value also is 0.13 m and probably not significant. The tidal difference between the two runs was small since they were only 14 minutes apart. In the overlap area the depth varied from 12 to 16 metres below the transducer, so that on this occasion the repeatability (to three standard deviations) was in the range $\delta Z/Z = \pm 0.028$.

Both surveys give similar results in these tests of repeatability. The absolute errors for any one run would depend upon knowledge of the mean sound speed, but this would be known accurately enough; it seems reasonable then to divide the variance measured above between the two crossing runs, indicating peak errors of the order of ± 2 % of the depth. The minimum angles θ used in the surveys were 13° and 8.8° respectively, and it is clear that larger errors can be expected when using smaller angles to achieve ranges out to ten times the depth. To do better would require much tighter control of α and careful monitoring of the sound profile for refraction.
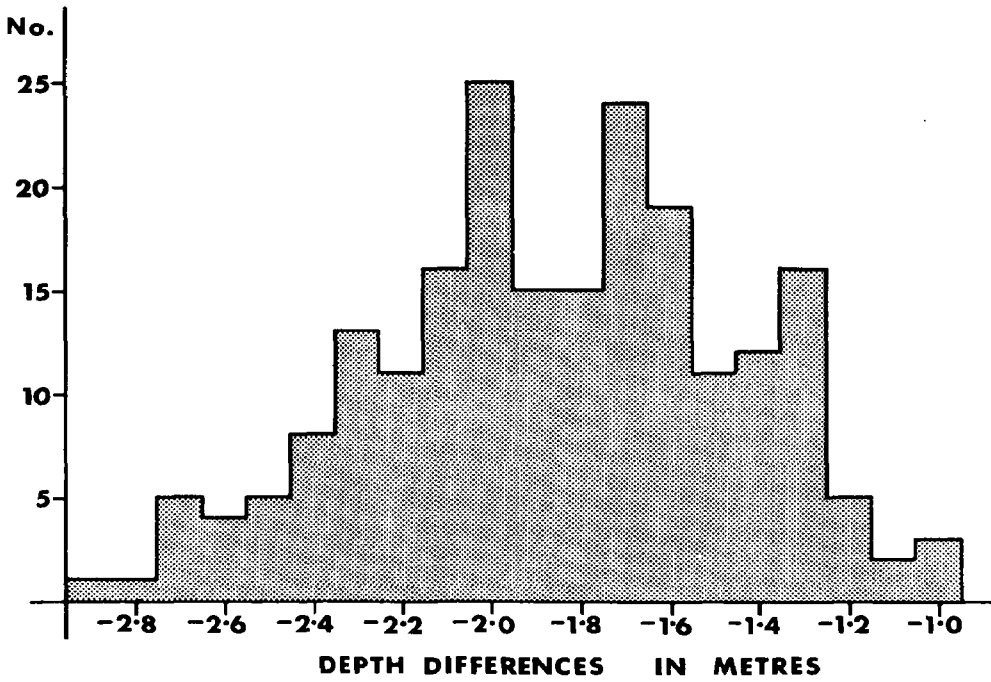
FIG. 14. — Histogram of depth differences for the Dodman Point Survey.
211 samples, mean error — 1.85 m, standard deviation 0.40 m, tidal correction — 2.2 m.
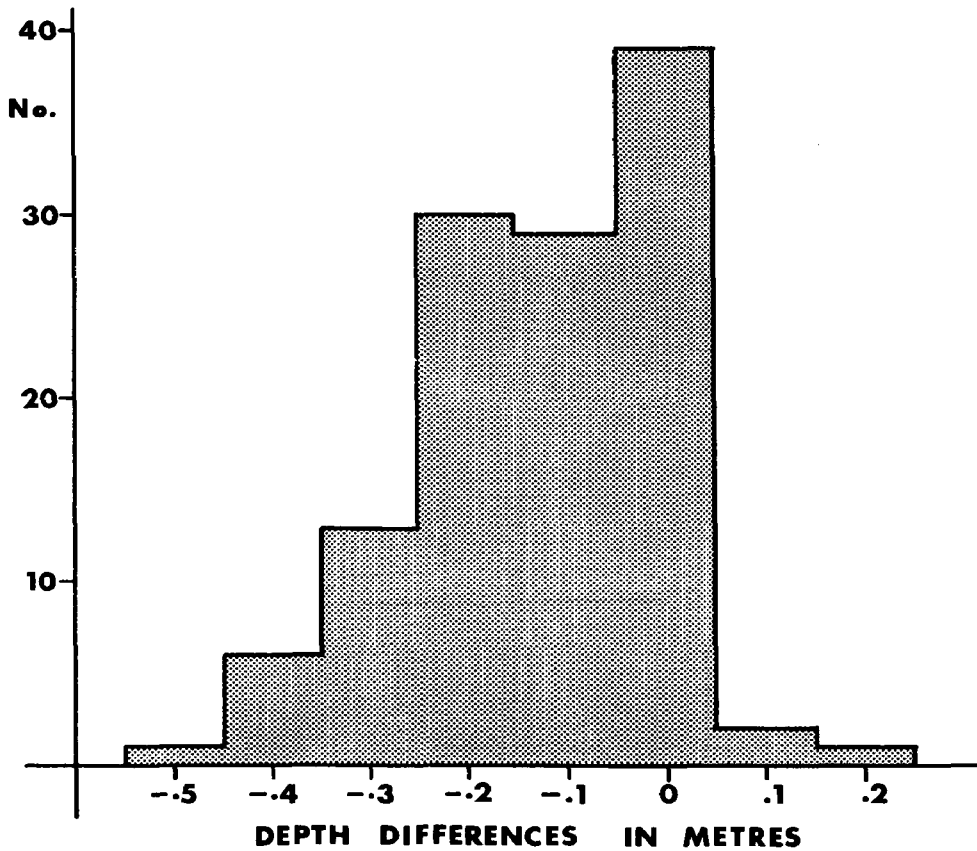
FIG. 15. — Histogram of depth differences for the Long Sand Head survey.
121 samples, mean error — 0.13 m, standard deviation 0.13 m, tidal correction nil.

SUMMARY

The use of an acoustic method to obtain wide swathe depth coverage from a survey ship is a logical extension of the echo-sounder and the term " Telesounder " is suggested for this type of instrument. In addition to the echo travel time it is essential to know the angle at which the sound is conveyed to and from the sea-bed, whose position is then available in polar co-ordinates from the transducer. The polar co-ordinates are converted to cartesian and related to the navigational data to produce a chart suitable for contouring. It is inevitable that the need for an extra co-ordinate should lead to further sources of error compared with an echo-sounder, and in practice the telesounder depth accuracy is determined by the angular accuracy one can achieve. *Thus the discussion on errors due to ship motions and sound refraction will apply whatever method is chosen to implement the telesounder principle.*

The telesounder system described in this paper is based upon a multiple beam side-scan sonar and has been operated at sea under realistic, if not exhaustive, conditions. The records reproduced here represent less than 0.5 % of the total obtained during two short cruises. The errors in depth over the swathe were generally less than 2 % but this figure should be regarded as 'typical' rather than necessarily the best one might achieve or the worst one might expect under some conditions.

The important parameters in designing this type of system are the frequency f, and hence wavelength, λ, transducer spacing, d, and α, the tilt angle.

The frequency will normally be as high as possible consistent with achieving the maximum range in order to restrict the transducer dimensions. The 250 kHz equipment described here was designed to measure to 200 metres range in typically 20 m water depth. Some longer range records have also been obtained at 36 kHz, for example fig. 16, by using the outer transducer rows of a side-scan sonar, for which $d/\lambda = 8.23$. Normally the length of the transducer will be about $40\,\lambda$, to give good resolution in the horizontal plane, and the width about $3\,\lambda/4$ to provide a reasonable envelope for the beam sensitivity.

The transducer spacing, d, in wavelengths determines the number of beams, N, and the beam angles, θ_n, and hence the number and interval of lateral samples. It also determines the beamwidths, which, for low N values, limit the depth accuracy; with higher values of N, errors in the tilt and roll angles tend to limit the depth accuracy, and also cause the near vertical beams to be lost with practical pulse lengths. This can be seen on many of the records and causes a gap in short range coverage, Fig. 12, though this is made much worse by the particularly weak sensitivity envelope, fig. 2, over this sector. N values between 25 and 50 are realistic.

FIG. 5. — An area of sea floor with steps in the Bristol Channel. Length 1000 m, width 250 m, water depth 15-30 m.
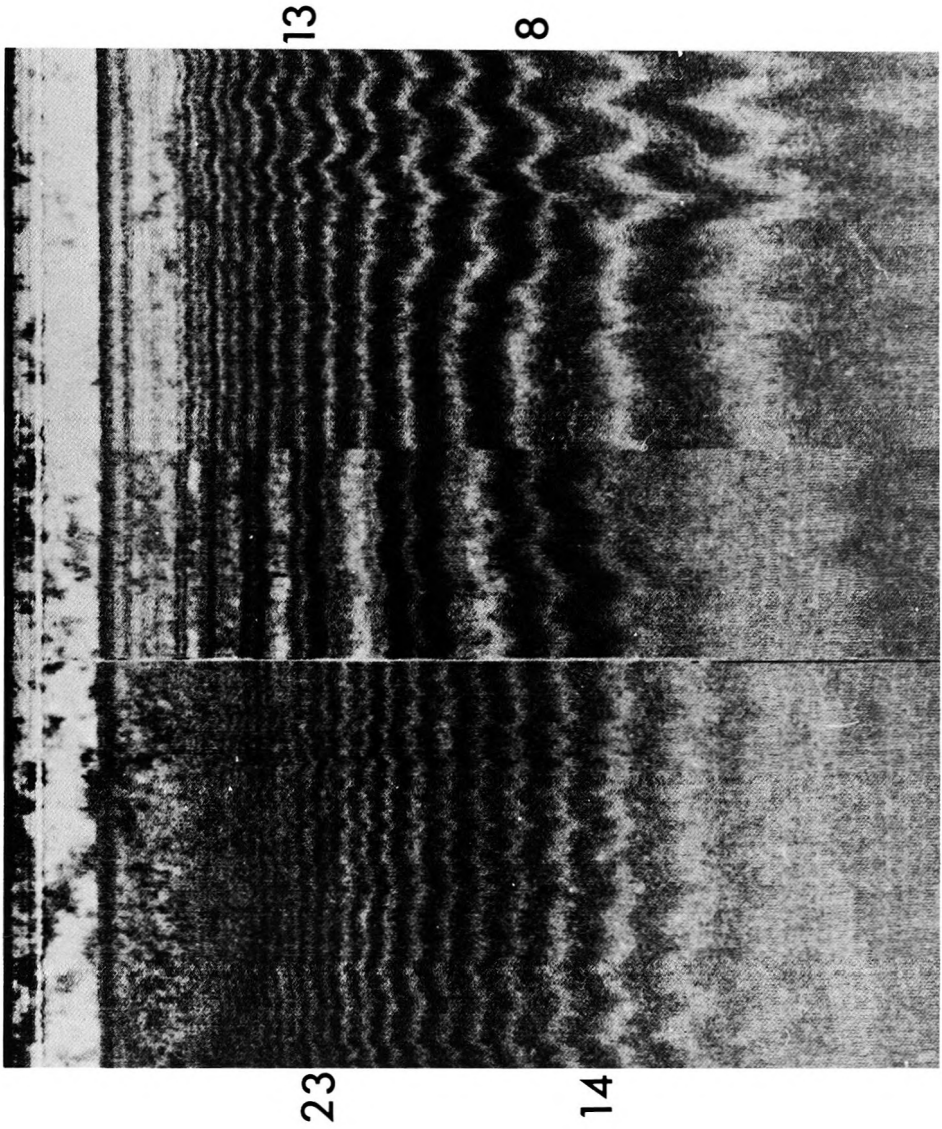
FIG. 6. — The effect of switching transducers. The patterns produced by transducers T_1 and T_2 are shown on the left and right respectively. The centre pattern is produced by the summation of T_1 and T_2. Length 650 m, width 200 m, water depth 20 m.
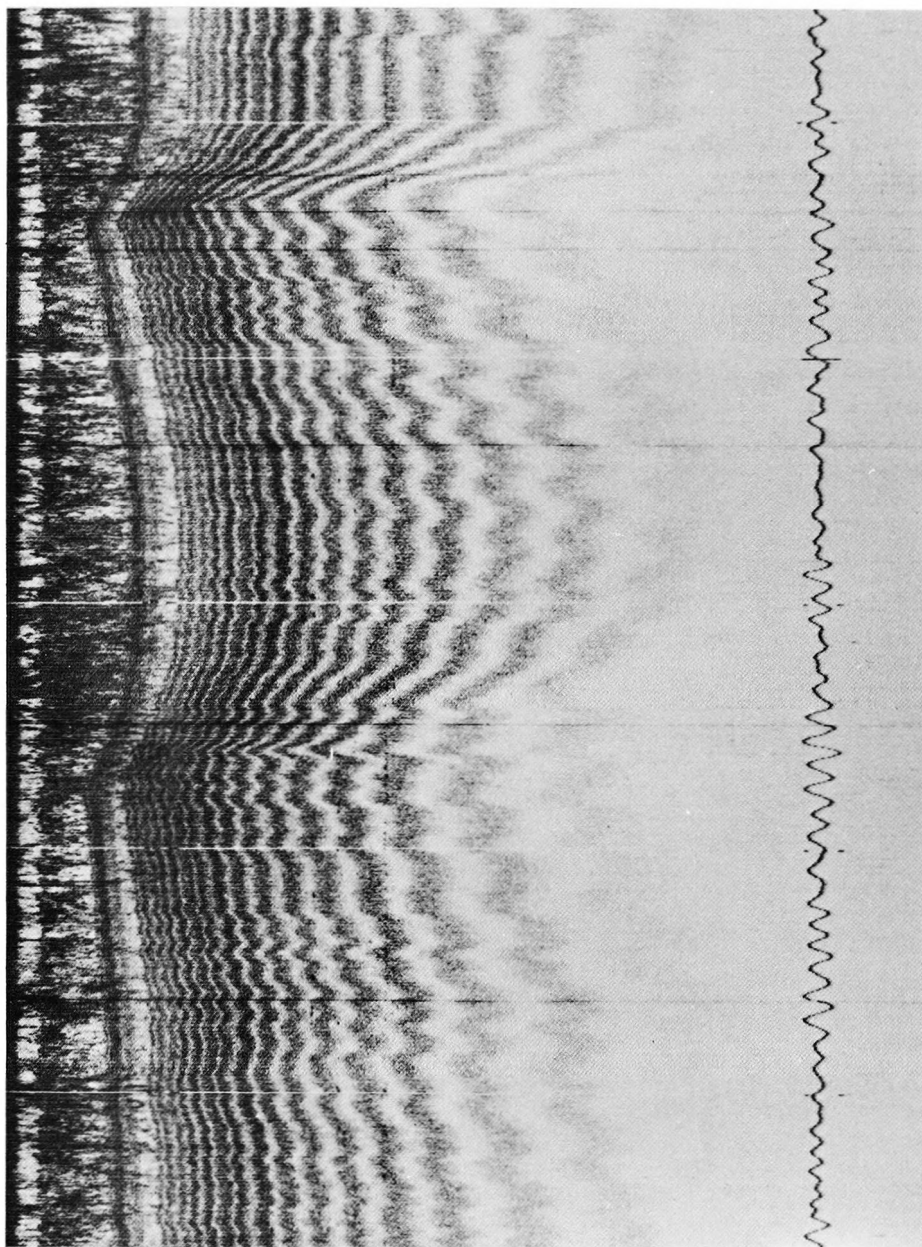
FIG. 7. — Two large sand waves off Selsey Bill in the English Channel. Length 1800 m, width 250 m, water depth 22-36 m.
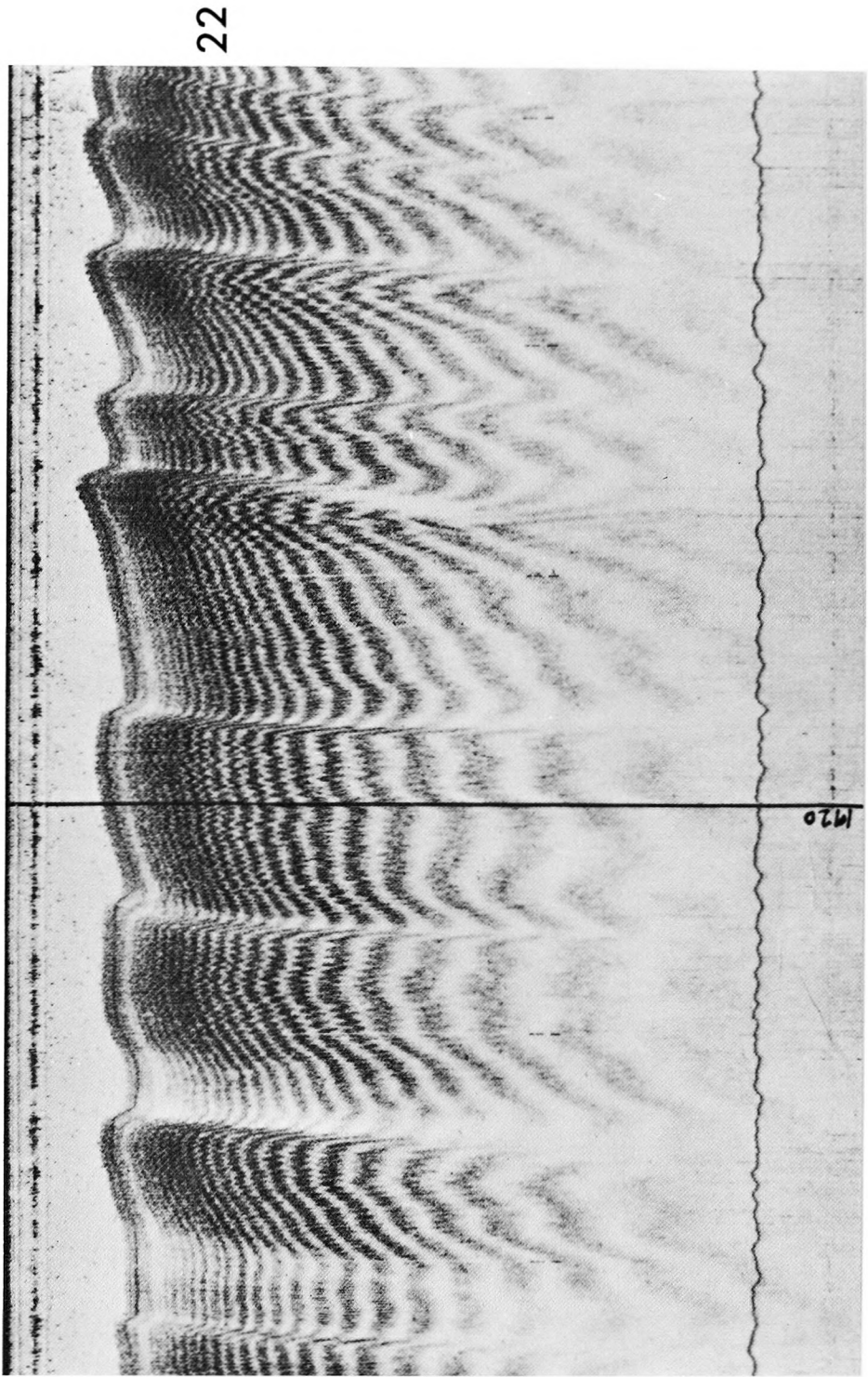
Fig. 8. — A series of asymmetric sand waves in the southern North Sea.
Length 2200 m, width 250 m, water depth 20-36 m.
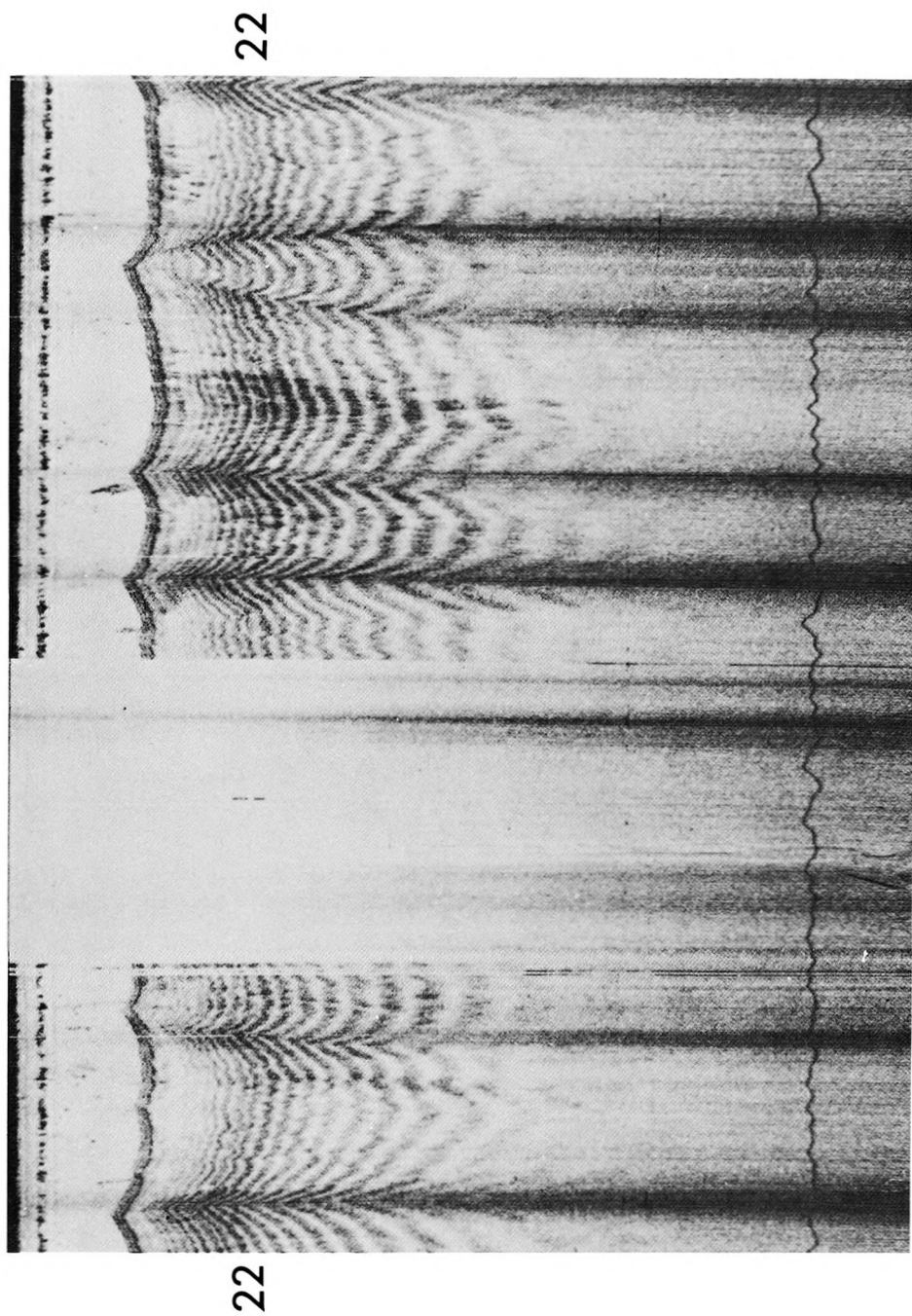
Fig. 9. — Regular sand waves and associated noise generated on the wave crests in the southern North Sea.
Length 1700 m, width 250 m, water depth 30-40 m.
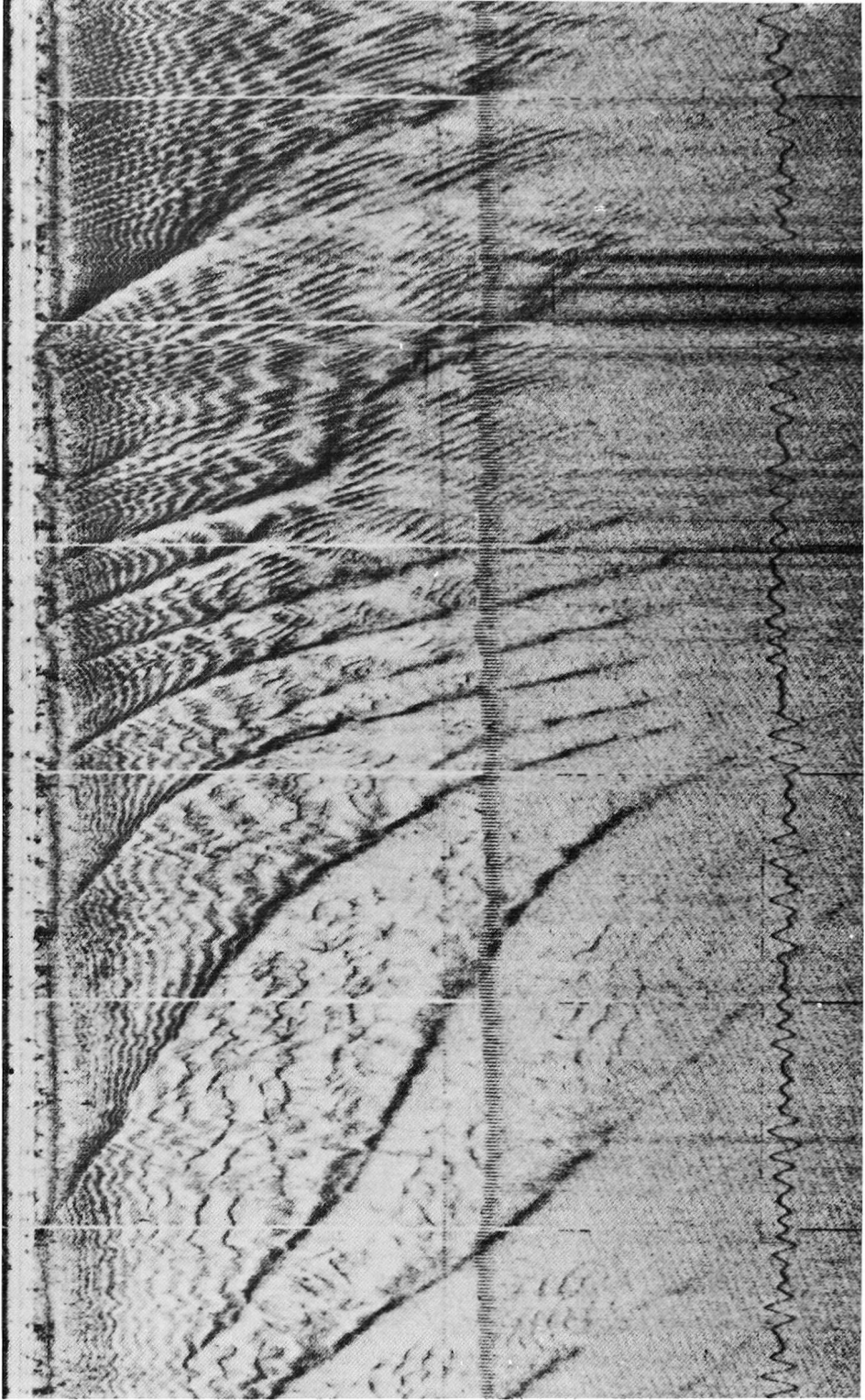
FIG. 10. — A complex sand wave region in the outer Thames Estuary. Length 1100 m, width 250 m, water depth 12-15 m.
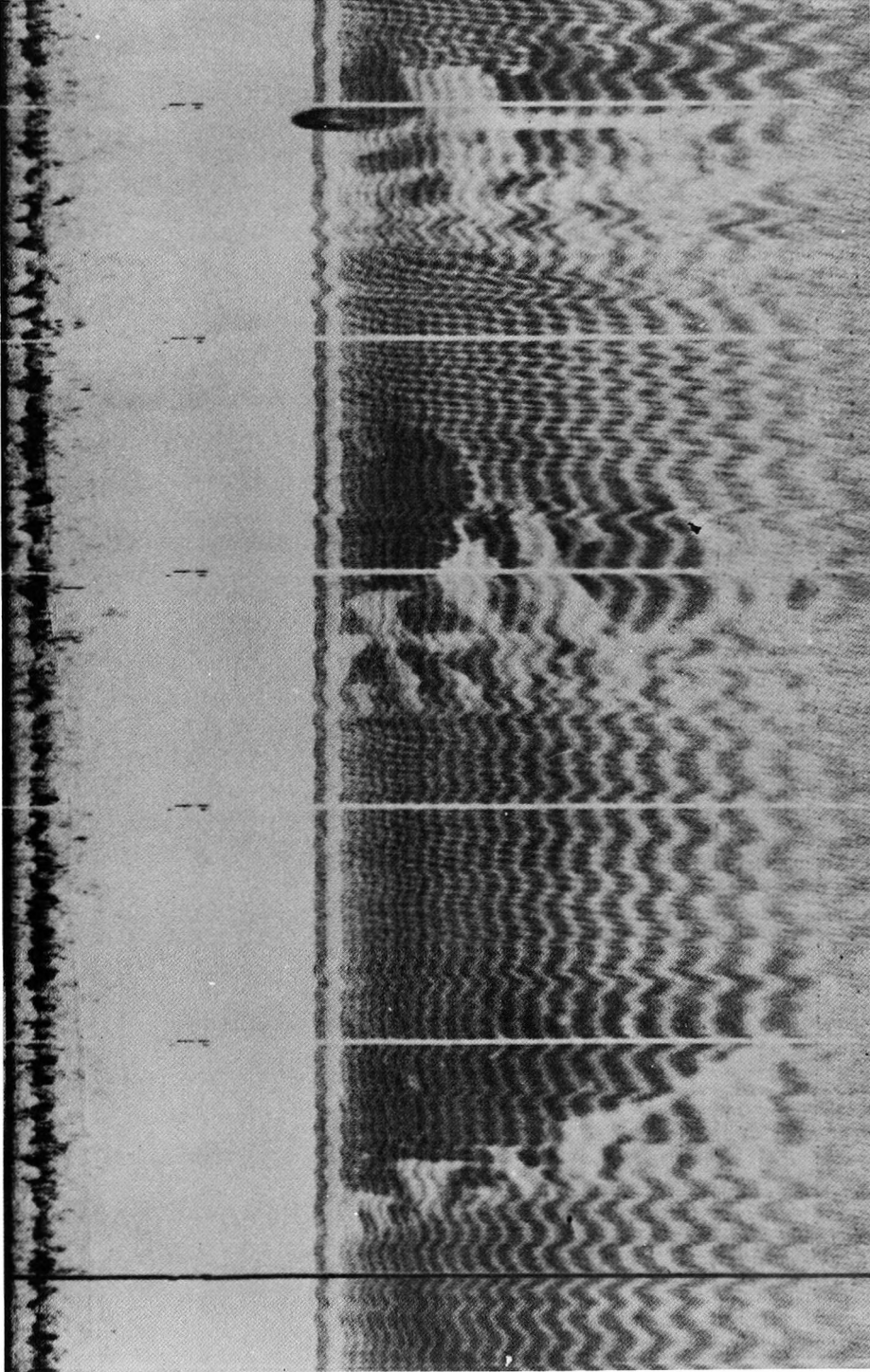
Fig. 11. — A flat sea floor composed of three types of area each having
different surface textures.
Length 1100 m, width 250 m, water depth 88 m.
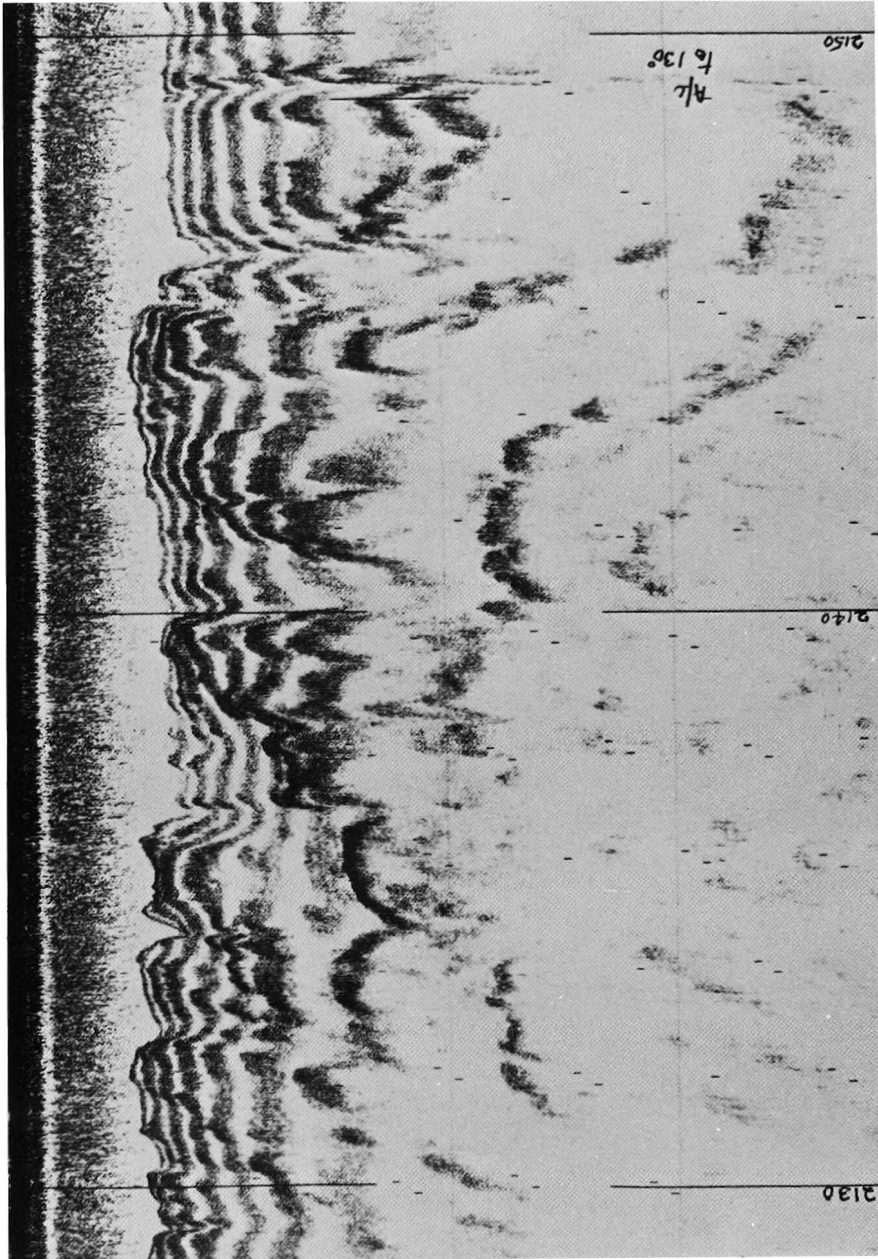
FIG. 16. — 36 kHz telesounder sonograph of a glaciated area in the Skagerrak. Length 7800 m, width 1000 m, water depth 140-230 m.

For quantitative work the angle, α, must be known accurately and this probably rules out telesounders in towed bodies, and calls for a ship mounted, roll stabilized platform. The only occasion on which a tele-sounder could be used without a stabiliser would be during absolute flat calm conditions but refraction could then be a greater problem. The period following a water mixing storm may be a good time to carry out telesounder surveys, so roll servomechanisms could be called upon to control within ± 10′ as the ship rolls ± 10°. If a roll gyro is not available for other purposes, its cost is liable to exceed that of the rest of the system.

The full analysis of records can be performed with general purpose data processing machines for short or occasional surveys. For longer or routine use some development of specialised data handling equipment may be necessary. With a telesounder on each side of the ship, and at the rate demonstrated in fig. 13, continuous surveying would produce over a million depth readings per day covering 100 square kilometres.

Telesounding could be useful in harbour, estuarine and inshore surveying. Its usefulness in general marine depth survey work depends upon how hydrographers trade off savings in ship time (or a greater coverage per working day) against the data handling problem and reduced quality of depth readings compared with the traditional echo-sounder. Scientific applications of telesounding within the limits described here already exist in marine geological studies on the continental shelf.

ACKNOWLEDGEMENTS

REFERENCES

ALBERS, V.M. (1965) : Underwater acoustics hand book II. The Pennsylvania State University Press, Pennsylvania, 1965.

BELDERSON, R.H., KENYON, N.H., STRIDE, A.H. and STUBBS, A.R. (1972) : Sonographs of the sea floor. Elsevier Publishing Company, Amsterdam, 1972.

CHESTERMAN, W.D., ST. QUINTON, J.M.P., CHAN, Y. and MATTHEWS, H.R. (1967) : Acoustic surveys of the sea floor near Hong Kong. *Int. Hyd. Rev.*, **44** (1), pp. 35-54.

CLOET, R.L. (1970) : How deep is the Sea ? *J. Inst. of Nav.*, **23** (4), pp. 416-425.

CROWTHER, P. (1973) : Personal communication.

DAINTITH, M.J. (1970) : A simple method of correction for refraction in underwater acoustic navigational systems. Paper presented at Brit. Acoust. Soc. meeting 19th May 1970, 6 pp.

ENGELMANN, I. (1967) : Towed echosounders for parallel sounding. *Int. Hyd. Rev.*, **44** (2), pp. 7-10.

FAHRENTHOLZ, S. (1963) : Profile and area echograph for surveying and location of obstacles in waterways. *Int. Hyd. Rev.*, **40** (1), pp. 23-37.

GLENN, M.F. (1970) : Introducing an operational multi-beam array sonar. *Int. Hyd. Rev.*, **47** (1), pp. 35-39.

GREISCHAR, L.L. and CLAY, C.S. (1972) : Use of side-scanning sonar for contouring bottom features. *J. Acoust. Soc. Am.*, **51** (3), pp. 1073-1075.

HAINES, R.G. (1963) : Developments in ultrasonic instruments. *Int. Hyd. Rev.*, **40** (1), pp. 49-57.

HAINES, R.G. (1970) : Searoom for the super-tanker. *Navy*, **75** (6), pp. 189-190.

HEATON, M.J.P. and HASLETT, W.G. (1971) : Interpretation of Lloyd Mirror in side-scan sonar. *Proc. Soc. for Underwater Technol.*, **1** (1), pp. 24-38.

(HICKLEY, T.J.) (1966) : Narrow-beam transducer sounding system. *Int. Hyd. Rev.*, **43** (1), pp. 37-42.

HOPKINS, J.C. (1970) : Cathode ray tube display and correction of side-scan sonar signals. *In :* Proc. I.E.R.E. Conf. Electron. Eng. Ocean Technol., Swansea 1970, pp. 151-158.

HOWSON, E.A. and DUNN, J.R. (1961) : Directional echo-sounding. *J. Inst. of Nav.*, **14** (3), pp. 348-359.

McKINNEY, C.M. and ANDERSON, C.D. (1964) : Measurements of back-scattering of sound from the ocean bottom. *J. Acoust. Soc. Am.*, **36** (1), pp. 158-163.

MITSON, R.B. and COOK, J.C. (1970) : Shipboard installation and trials of an electronic sector scanning sonar. *In :* Proc. I.E.R.E. Conf. Electron. Eng. Ocean Technol., Swansea 1970, pp. 187-210.

RITCHIE, G.S. (1970a) : British Hydrography since Cook. *The Naval Review*, **58** (1), pp. 126-134.

RITCHIE, G.S. (1970b) : Problems in bathymetric surveying presented by modern trends in ship building. *The Radio and Electronic Engineer* , **40** (5), pp. 219-224.

Tucker, D.G. (1960) : Directional echo-sounding. *Int. Hyd. Rev.,* **37** (2), pp. 43-53.

Tucker, M.J. (1961) : Beam identification in multiple beam echo-sounders. *Int. Hyd. Rev.,* **38** (2), pp. 25-32.

van Weelde, H.H. (1972) : Deep draught surveys in the southern North Sea. *Hyd. Newsletter,* Netherlands, **5** (2), pp. 355-368.

Voglis, G.M. and Cook, J.C. (1966) : Underwater applications of an advanced acoustic scanning equipment. *Ultrasonics,* **4** (1), pp. 1-9.

Voglis, G.M. and Cook, J.C. (1970) : A new source of acoustic noise observed in the North Sea. *Ultrasonics,* **8** (2), pp. 100-101.

(Manuscript submitted in English)